CRACK BEHAVIOUR UNDER CREEP AND CREEP-FATIGUE CONDITIONS OF NICKEL-BASE SUPERALLOY MAR-M 247

J.-M. Rudnig, F. Mueller, A. Scholz, C. Berger
Institut für Werkstoffkunde (IfW), Technische Universität Darmstadt,
Grafenstr. 2, 64283 Darmstadt, Germany

ABSTRACT

The crack initiation time and crack growth rate were determined in [1] for aero engine and stationary gas turbine engine blade material nickel-base-superalloy MAR-M 247. Long-term tests (up to 3 000h) at 850°C in conventional cast and 950°C in directionally solidified condition had been performed. Creep-, fatigue- and creep-fatigue loading were applied. Component similar corner-crack-specimens had been examined. The crack starter notch had been applied using the razor-blade method, which provides a crack tip radius of less than 10 µm.
Crack initiation times and growth rates had been correlated with the stress intensity factor K_I. Additionally, the results of tests obtained on special designed cross drilled tubular specimens, simulating the cooling drills in real turbine blades, were compared with the results on corner-crack specimens. This allows an evaluation of the transferability of test results obtained on standard fracture-mechanic specimens to components subjected to creep-, fatigue- and creep-fatigue interaction.

KEYWORDS

high temperature crack behaviour, creep and/or creep-fatigue conditions, crack initiation, crack growth, corner-crack-specimen, nickel-base-superalloy, MAR-M 247

INTRODUCTION

A high power density is an important criterion of competition for gas turbines. Due to the high temperatures and high loads, especially in turbine blades, nickel-base superalloys became the most important group of materials in this field of application. The use of directionally solidified nickel-base superalloys instead of conventionally cast material allows higher temperatures and even higher stresses and therefore leads to an additional increase in performance and efficiency.
To achieve a higher economic use of material and production technology, small notches, defects and flaws can not be avoided and should be tolerated along production and service maintenance.
However, these defects may be subject to crack initiation and crack propagation under long-term service conditions. To study these problems and to support an advanced remnant life evaluation, fracture mechanics procedures are required.
Due to the variable loading conditions of aero engine turbines as well as modern power plant gas turbines, creep-fatigue crack behaviour becomes more decisive for life assessment and integrity of components.

MATERIAL, SPECIMEN AND TESTING

Material

Jet and stationary turbine engine blade nickel-base-superalloys MAR-M 247 CC (conventional cast) and MAR-M 247 LC DS (low carbon, directionally solidified) were investigated. Both materials were produced by Doncaster Precision Castings in Bochum, Germany among industrial material specifications.

After vacuum melting, casting and solidification, the materials were treated with a precipitation hardening process, consisting of multiple phases of inert annealing and quenching. The longitudinal sections through both materials are shown in **Fig. 1**. The grain size within the specimen extracting position (radius of ca. 8 mm from the centre of the bar in cross section) was determined to 0.7mm for the CC and 0.8mm for the DS version.

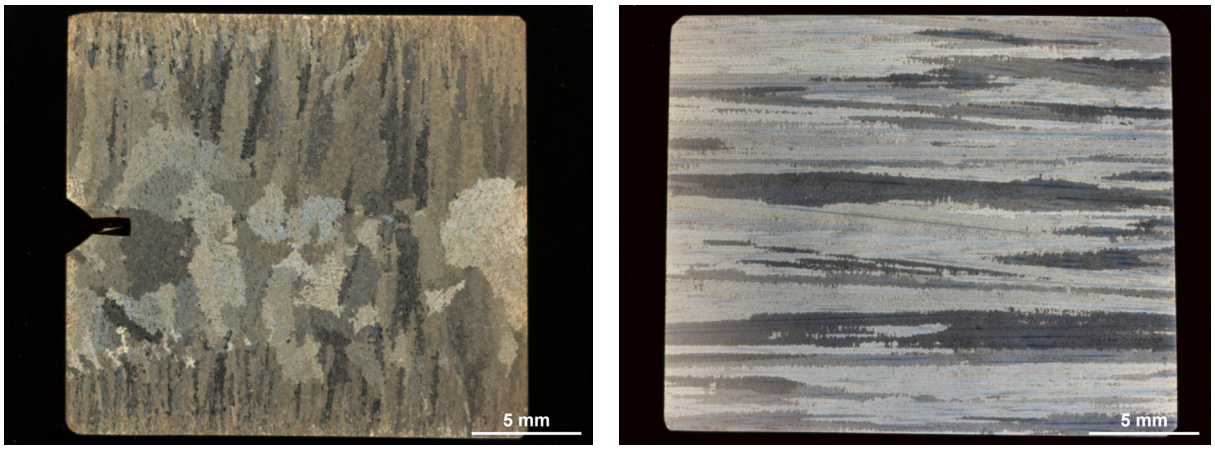

Figure 1: Longitudinal section through material MAR-M 247 CC (left) and MAR-M 247 LC DS (right), condition as supplied, etched for visualisation of grain structure

Specimen Types and Preparation

For both materials, tests were performed on corner-crack-specimens (**Fig. 2**) with a cross section of 8x8mm. Additional tests obtained on special designed cross-drilled tubular hollow-specimens made of MAR-M 247 LC DS, complying cooling drills in turbine blades, allow an evaluation of the transferability of test results obtained on corner-crack-specimens to the component.

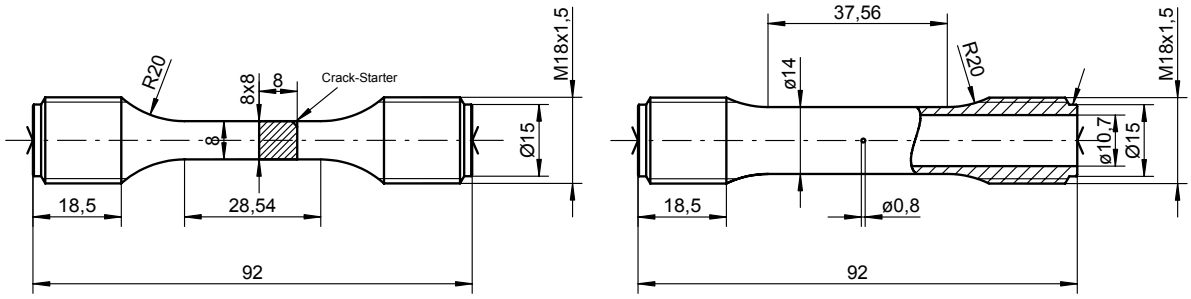

Figure 2: Specimen geometries: corner-crack- (left) and cross-drilled hollow-specimen (right)

For machining of the crack-starter-notch into the corner-crack-specimens, the “Razor-Blade-Method” had been applied (**Fig. 3**). Known from the ceramic research sector [2], the crack-starter-notch will be grinded into the specimen with a sharp razor-blade and some diamond-suspension (graining 1µm) by oscillating movement. Due to the desired total depth of the starter-notch (1.1mm), the Razor-Blade-Method was applied into the base of a notch pre-machined to a depth of 1mm by EDM (Electrical Discharge Machining). Only the last 0.1mm was grinded by the razor blade.

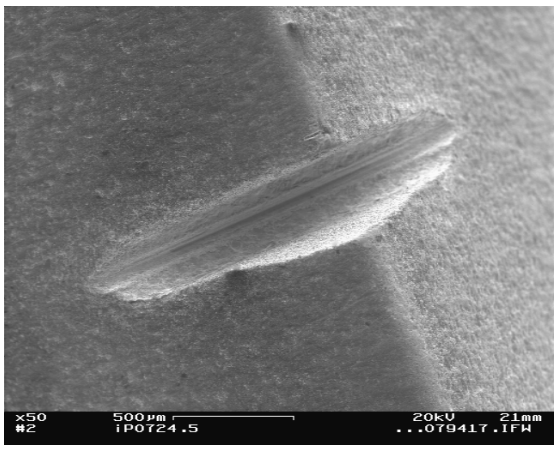

Figure 3: Crack-starter-notch, SEM-image

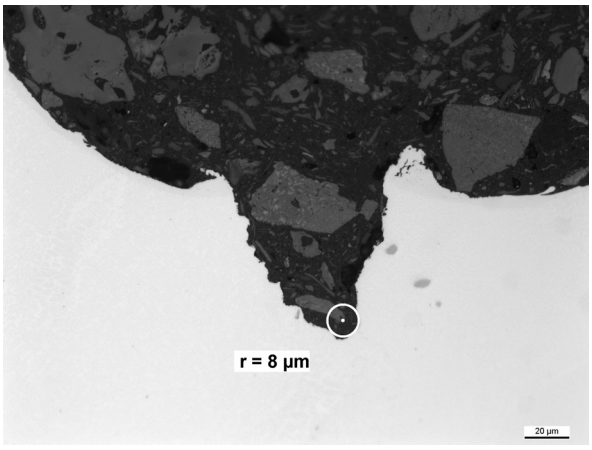

Figure 4: Measurement of crack-zip-radius

A crack-starter-notch among ASTM 1457-07 [3] must have a minimum diameter of 0.1mm which complies to a crack tip radius of ca. 50µm. A small crack tip radius leads to a realistic representation of the stress situation at the crack tip and implies an ideal initial situation for the experiment. Notches machined by razor-blade achieve a typical crack tip radius of ca. 10µm (**Fig. 4**). Due to this fact, it might be possible to resign of pre-fatigued crack-starter-notches, which are known to be obligate in low-ductile nickel-base-superalloys. The cross-drills with a diameter of 0.8mm in the tubular hollow-specimens were machined through both sides of the specimen by EDM-die-sinking.

Test-Parameters and Matrix

All tests were performed with the “t_{R1}-t_{H1}-t_{R2}-t_{H2}” test-cycle shown in **Fig. 5**. Fatigue-tests were performed with 1-1-1-1s, creep-fatigue-crack-tests with 1-300-1-1s, featuring a hold-time of 300s at maximum load.

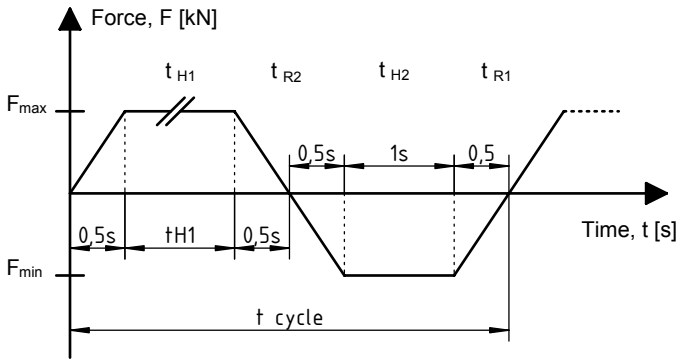

Figure 5: Test-cycles for fatigue and creep-fatigue-tests with hold-time t_{H1}

Creep- and creep-fatigue-crack-tests have been performed on corner-crack-specimens made of MAR-M 247 CC at 850°C and the directionally solidified version MAR-M 247 LC DS at 950°C. Test durations were up to 3 000h both for static and creep-fatigue-loading on each material. Additionally, 90 000 cycles fatigue- and 3 500 cycles creep-fatigue-crack-tests were implemented on cross-drilled-hollow tubular-specimens made of MAR-M 247 LC DS. **Tab. 1** shows details of the test matrix concerning to the presented results.

Material	Test Type	Specimen	T [°C]	R	Cycle [s]	σ_{max} [MPa]
MAR-M 247 CC	Creep	Corner-Crack	850	1	∞	380
						290
	Creep-Fatigue			-1	1-300-1-1	270
						195
	Fatigue	Corner-Crack (without Notch)			1-1-1-1	270
MAR-M 247 LC DS	Creep	Corner-Crack	950	1	∞	188
						135
	Creep-Fatigue			-1	1-300-1-1	170
		Drilled Hollow			1-300-1-1	105
	Fatigue				1-1-1-1	120

Table 1: Test Matrix

Experimental Setup

The creep-crack-tests were effected on electromechanical testing machines, the cyclic fatigue- and creep-fatigue-crack-tests on a servo-hydraulic test machine using a MTS control system. Both machine types are using convection-furnace systems with three individually controlled sections, ensuring constant temperature along the entire specimen.
Axial- (for creep-tests) and side-extensometers (for fatigue- and creep-fatigue-tests) were used to measure the load-line-displacement (LLD). For determination of crack-initiation and crack-propagation, AC-potential-drop-systems (ACPD) of types “MATELECT CGM5” and “CGM7” were used (**Fig. 6**). At the end of the test, the specimens were brittle-fractured and the measured potential-drop signals were correlated with the initial and the maximal crack length for each specimen.

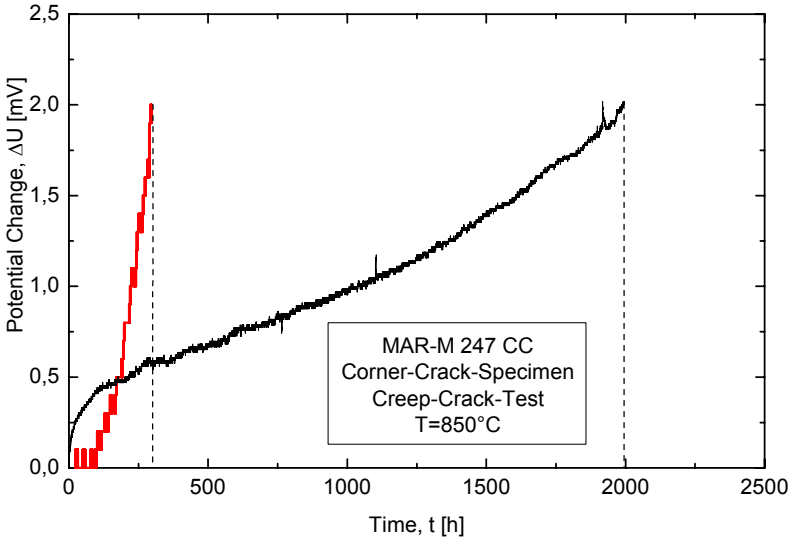

Figure 6: AC-potential-drop vs. time, creep-crack-tests

RESULTS AND DISCUSSION

The crack initiation behaviour (times and cycles for a technical crack-length ∆a=0.2mm) and propagation rates were correlated with the stress intensity factor K_I (**Eq. 1**).

$$K_I = \sigma_N \cdot (\pi \cdot a)^{1/2} \cdot f \quad (1)$$

The geometry-functions (f) for the corner-crack-specimens (quarter elliptical crack in a disk under constant stress condition) are taken from [4].

Due to the intergranular creep-crack-growth and the relatively coarse-grained structure on MAR-M 247 CC, the crack-front was formed inhomogeneously under creep-conditions (**Fig. 7**). At the following facture-mechanic evaluation, the maximum crack-length a_{max} was used for conservative assessment. However, it should be noticed that due to the very distinct inhomogeneity of the crack front, the validity-criteria for K_I and C* [3] are not fulfilled.
Under creep-fatigue- and fatigue-load the crack-fronts (**Fig. 8**) are homogenous, transgranular and shaped quarter elliptical.

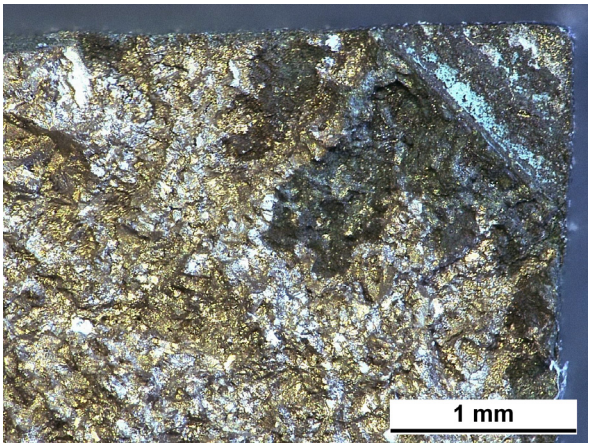

Figure 7: Crack-Front after Creep-Loading, MAR-M 247 CC

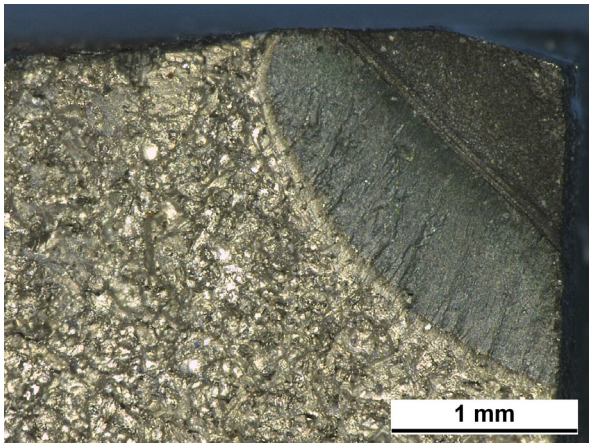

Figure 8: Crack-Front after Creep-Fatigue-Loading, MAR-M 247 CC

At creep-fatigue conditions on MAR-M 247 LC DS, phenomena like propagation preferences in certain crystallographic orientations, crack-stop or crack-branching can be explained through grain-boundaries and orientation-misfits between different grains (**Fig. 9**).
A correlation between the crack path in the specimen and the microstructure of the material was investigated using Electron Backscatter Diffraction (EBSD). Grain-structures, -sizes and -boundaries can be identified and located due to their different orientation.
Figure 9 shows two cracks transverse to the load axis, having its source at the cross drill of a hollow specimen made of MAR-M 247 LC DS. The creep-fatigue crack path shows a crack stop-phenomenon on a grain boundary with multiple branching (left side crack). The adjacent grains show a maximum misfit in orientation to each other, 111 vs. 101 direction (001 is the direction of solidification). The crack branches and defuses to reduce stress intensity at the crack-tip rather than proceeding through the boundary.

The crack-initiation behaviour of the conventional cast MAR-M 247 for a technical crack length of ∆a=0,2mm is shown in **Fig. 10**. The introduction of cycles leads to a decrease of crack initiation time. **Fig. 11** shows the comparison of creep-crack-growth rates (da/dt) for MAR-M 247 CC and DS. Due to the higher test-temperature, the DS-material shows a higher creep-crack-growth rate.

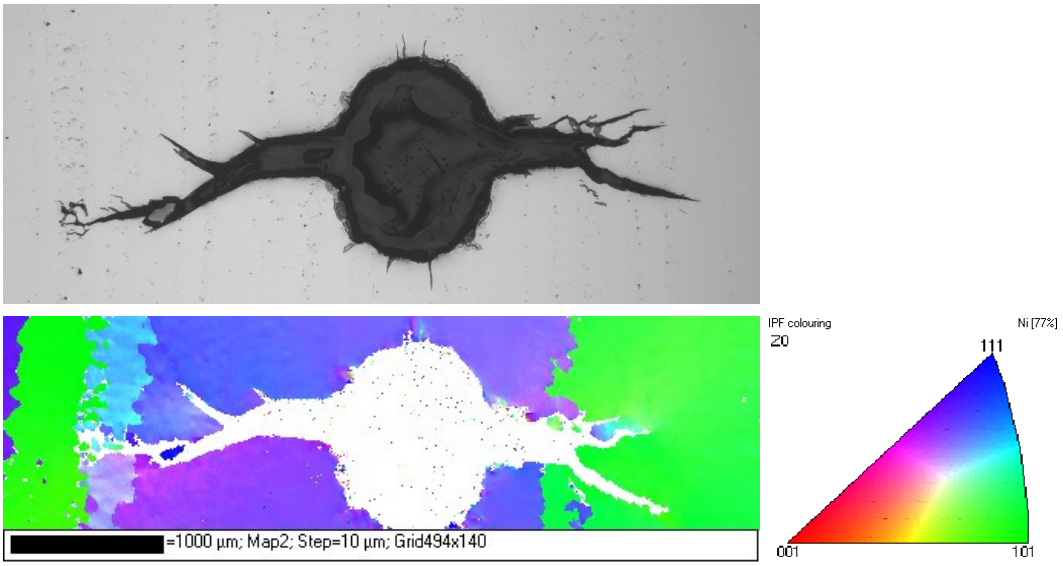

Figure 9: Map of crystallographic orientation measured by EBSD, MAR-M 247 LC DS, creep-fatigue crack, t_H=300s

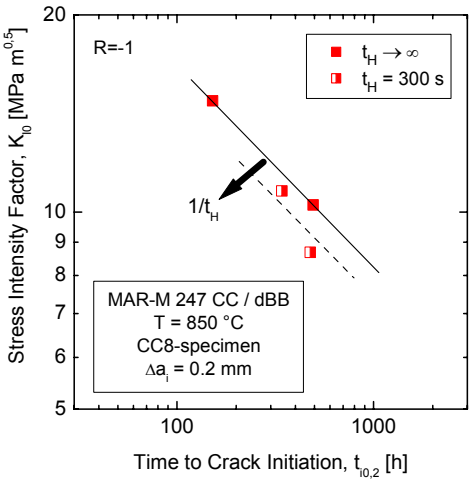

Figure 10: Crack-initiation-time vs. stress-intensity-factor K_I

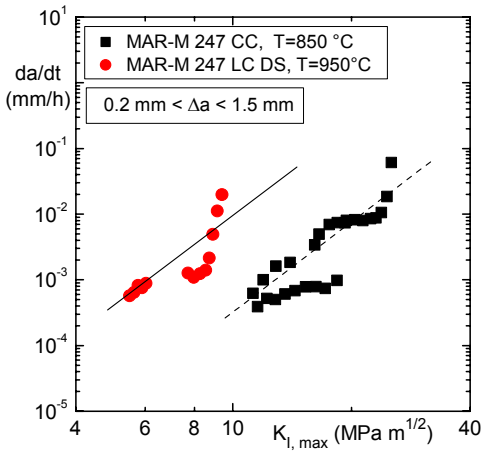

Figure 11: Comparison of creep-crack-growth-rate for MAR-M 247 CC and DS

The test-duration-time of corner-crack-specimens made of the DS-alloy are compared with the creep-rupture-strength determined on smooth specimens in **Fig. 12**. The 1%-strain-limit, $R_{p1,}$ was calculated from the creep-rupture-strength among [5], which defines a decrease in stress of ca. 9.1% from R_u to R_{p1} to be appropriate. The 1%-strain-limit was extrapolated to higher times. The creep-crack-initiation on corner-crack-specimens occurs near the 1%-strain-limit R_{p1}. **Fig. 13** shows the cross section of the crack-starter-notch of a corner-crack-specimen made of Mar-M 247 LC DS. The specimen shows extensive blunting but no creep-crack-initiation at all after 1 600h creep-test and a measured total permanent strain of 1.1%.

Typical terms of design only allow a maximum strain of less than 1% for a gas turbine blade before it has to be replaced [5]. The test-results on corner-crack-specimens confirm that a fracture-mechanic assessment of gas turbine blades made of MAR-M 247 LC DS under creep-load might be unnecessary.

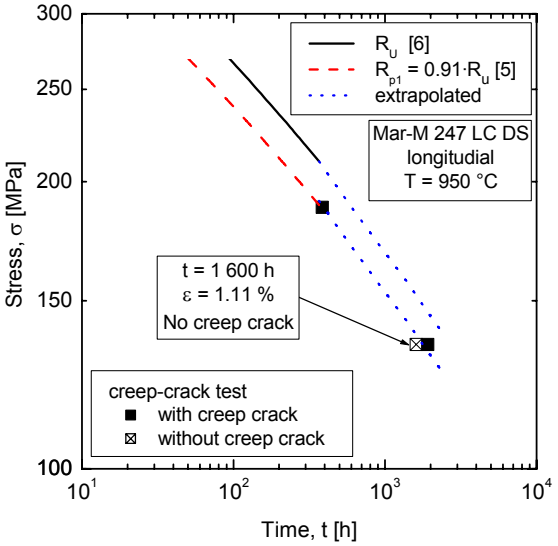

Figure 12: Comparison of test duration of corner-crack-specimens with R_u and R_{p1} for MAR-M 247 LC DS

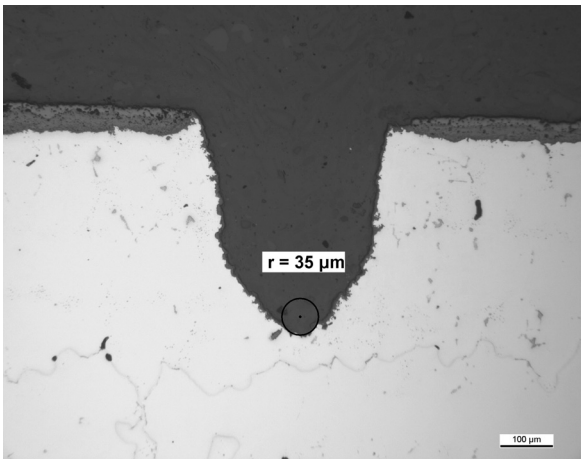

Figure 13: Crack-starter-notch, corner-crack-specimen, MAR-M 247 LC DS, after 1 600h creep-test at 950°C, cross-section

The creep and creep-fatigue crack-growth-rates vs. stress intensity factor K_I for MAR-M 247 LC DS are shown in **Fig. 14**. The alloy shows a clear hold-time-dependence of the creep-fatigue crack-growth-rate. Experimental values for t_H=300s are significantly higher than for pure creep conditions. With decreasing hold-time, an increase of the crack-propagation per cycle is observed. The crack-growth under creep-fatigue-conditions can alternatively be described by depicting the crack-propagation per cycle da/dN against the range of stress intensity ΔK_I. Such results are compared to the results of fatigue-crack tests in **Fig. 15**. The scatter band for fatigue crack-growth is valid for R=0,01 to 0,05 and T=400 to 760°C.

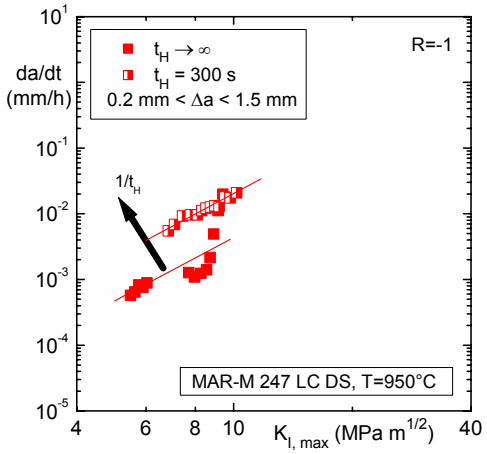

Figure 14: Creep-fatigue-crack-rate vs. K_I, MAR-M 247 DS

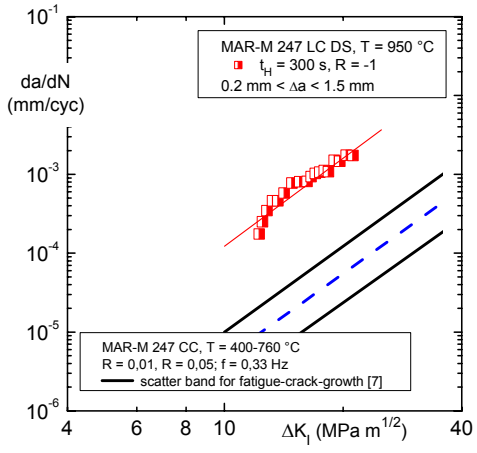

Figure 15: Creep-fatigue-crack-propagation MAR-M 247 DS, comparison with literature

The creep-fatigue-crack-growth rates obtained on the cross-drilled hollow-tubular-specimens are shown vs. the rage of stress intensity ΔK_I in **Fig. 16** and vs. the range of net stress $\Delta\sigma_{net}$ in **Fig. 17**. Using ΔK_I, the measured crack-propagation-rates on corner-crack-specimens are higher than the crack-propagation-rates measured on component similar cross-drilled hollow-

specimens. Using the range of net stress $\Delta\sigma_{net}$, the crack-propagation-rates in hollow-specimens are higher than in corner-crack-specimens. Therefore, it is recommended to use K_I for conservative fracture-mechanic assessments.

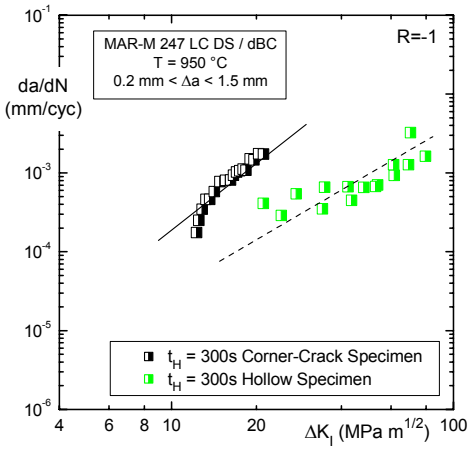

Figure 16: Creep-fatigue-crack-growth vs. ΔK_I, MAR-M 247 LC DS

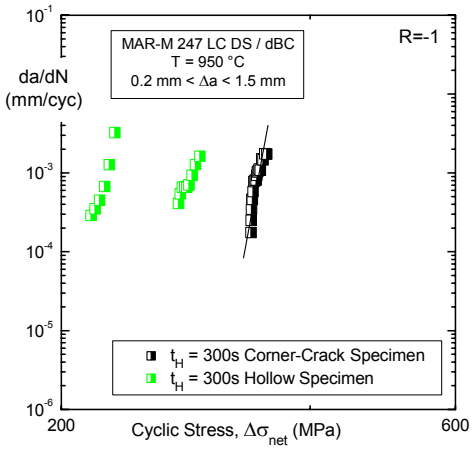

Figure 17: Creep-fatigue-crack-growth vs. $\Delta\sigma_{net}$, MAR-M 247 LC DS

Accumulation of Creep-Fatigue-Crack-Initiation and -Propagation

The accumulative description of creep-fatigue-crack-propagation on the basis of pure creep and fatigue contents had been performed successfully for steels [8] and for a nickel-base forged alloy. In this work, it can be shown that the crack initiation and propagation of the nickel-base cast superalloy MAR-M 247 under creep-fatigue-conditions can be recalculated by a linear accumulation of increments of pure creep-crack and fatigue-crack-data. Crack initiation can be assessed using damage accumulation (**Eq. 2**) until the crack initiation criteria L=1 is fulfilled.

$$\frac{t}{t_i}[K_I] + \frac{N}{N_i}[\Delta K_I] = L \tag{2}$$

This requires crack initiation data (e.g. for a technical crack length of Δa=0.2mm) for creep-loading $t_i(K_I)$ and fatigue-loading $N_i(\Delta K_I)$ load. The actual test-time t and test-cycles N will be added as the fraction to their initiation data (t_i and N_i).
After crack initiation criteria has been fulfilled, the calculation of crack propagation (**Eq. 3**) will be performed in incremental steps using the creep- and fatigue-crack-propagation-rates.

$$\left(\frac{da}{dN}\right)_{creep-fatigue} = \left(\frac{da}{dN}\right)_{fatigue} + t_H \cdot \left(\frac{da}{dN}\right)_{creep} \tag{3}$$

$$\frac{da_{creep}}{dt} \cdot \Delta t_j = \Delta a_{creep,j} \tag{4}$$

$$\frac{da_{fatigue}}{dN} \cdot \Delta N_j = \Delta a_{fatigue,j} \tag{5}$$

$$\Delta a_{total,j} = \Delta a_{creep,j} + \Delta a_{fatigue,j} \tag{6}$$

For the first propagation step, the starting crack length is the starter notch depth a_0 plus the crack-initiation length Δa_i referring to the criteria of the crack initiation data used for accumulation (e.g. 0.2mm: $t_{i0,2}$, $N_{i0,2}$). K_I (e.g. ΔK_I) is known from the previous step. Multiplication of the creep crack propagation rate da/dt (belonging to the K_I) with the Δt of the incremental step leads to the creep crack propagation part Δa_{creep} in this step (**Eq. 4**). Similar to this, multiplication of the fatigue crack propagation rate da/dN (belonging to the ΔK_I) with the ΔN of the incremental step leads to the fatigue crack propagation part $\Delta a_{fatigue}$ in this step (**Eq. 5**). Accumulation of creep- and fatigue-parts leads to the total crack propagation for creep-fatigue-load in this step (**Eq. 6**). Next step starts with same procedure but different K_I e.g. ΔK_I, determined from the crack length at the end of the previous step.

$$a_k = a_0 + \Delta a_i + \sum_{j=1}^{k} \Delta a_{total,j} \tag{7}$$

The accumulation of the incremental steps calculated with the method mentioned above leads to a description of the total crack-length at a certain step, respectively time or cycle (**Eq. 7**). The calculation of crack-length for a creep-fatigue-crack-test (corner-crack-specimen, MAR-M 247 CC) shows an acceptable accordance to the measured crack length (**Fig. 18**).

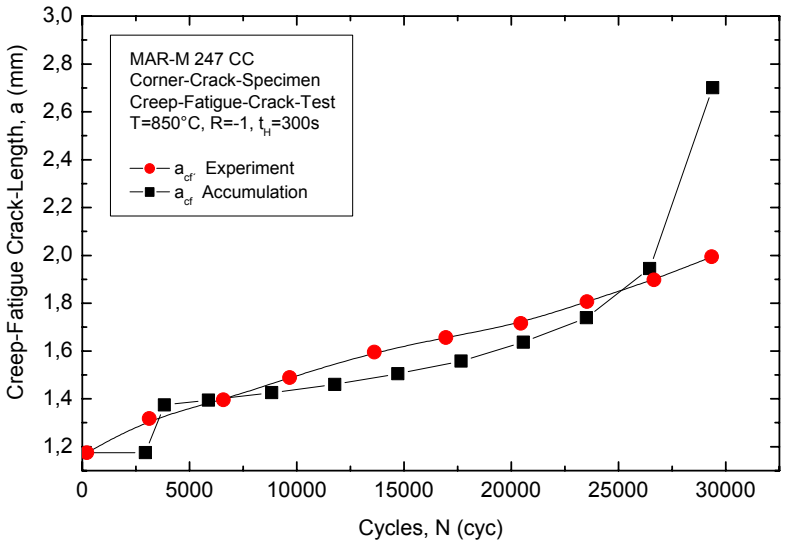

Figure 18: Experimental value $a_{cf'}$ and predicted value a_{cf} of creep-fatigue crack-length in function of cycles for an individual test on a corner-crack-specimen

SUMMARY AND CONCLUSIONS

The aims of this work are the determination and description of the creep-, fatigue- and creep-fatigue-crack-behaviour of nickel-base cast alloy MAR-M 247. The crack-initiation-time and the crack-growth-rate were determined in long-term regime at 850°C in conventional cast and 950°C in directionally solidified condition. Creep-, fatigue- and creep-fatigue-crack-tests have been performed until 3 000h test duration on corner-crack-specimens. The crack-starter-notch had been applied using the “Razor-Blade-Method”.
Crack-growth-rates and initiation times had been correlated with the stress intensity factor K_I. Additionally, tests obtained on special designed cross-drilled hollow-tubular specimens allow an evaluation of the transferability of test results obtained on fracture-mechanic specimens to the component.

Crack-initiation occurs under creep-fatigue conditions earlier compared to creep-load and under fatigue earlier compared to creep-fatigue. Crack-initiation can be detected under creep conditions for both materials at or above 1% total permanent strain. These test-results allow the conclusion that a fracture-mechanics assessment of gas turbine blades under creep-load might be unnecessary.
Introducing a 300s hold-time leads to an increase of crack-growth rate. Fatigue-crack propagation shows higher crack propagation rate than creep-fatigue with hold times of 300s. For conservative assessment of crack initiation and propagation for components, it is recommended to use the stress intensity factor K_I.
A model for the calculation of crack initiation and propagation under creep-fatigue-load was adapted to cast nickel-base superalloy MAR-M 247. The calculated crack propagation was compared with experimental data for creep-fatigue-tests obtained on corner-crack-specimens made of MAR-M 247 CC.

ACKNOWLEDGEMENT

The work and the results presented in this paper originate from the government-funded research-project [1] (AiF-No 15626, FVV No 962). Special thanks are dedicated to the supporting industrial enterprises for supplying the materials.

REFERENCES

[1] Berger, C., Roos, E., et.al.: Rissverhalten von Nickelbasis-Gusslegierungen mit unterschiedlicher Kornstruktur, Current Research Project AiF-Nr. 15626, IfW Darmstadt and MPA Stuttgart, 06/2008 – 05/2010

[2] Weiler, L.: Private Communication, Fachbereich Material- und Geowissenschaften, Fachgebiet Nichtmetallisch Anorganische Werkstoffe, Technische Universität Darmstadt, 2007

[3] ASTM E 1457-07. Standard Test Method for Measurement of Creep Crack Growth Rates in Metals, 2007

[4] Newman, J. C. Jr., Raju, I. S., Stress-intensity-factor equations for cracks in three-dimensional finite bodies, in Fracture Mechanics: 14th Symposium, Vol. I: Theory and Analysis, ASTM STP 791, pp. I-238-I-265, 1983

[5] Braeunling, W. J. G., Flugzeugtriebwerke, 3. Edition, Springer Verlag Dordrecht Heidelberg London New York, 2009

[6] Kloos, K.H., Granacher, J., Pfenning, A.: Rechnerische Beschreibung des Kriechverhaltens ausgewählter hochwarmfester Legierungen Teil 1: Kriechgleichungen für einzelne Versuchswerkstoffe, Materialwissenschaft und Werkstofftechnik, Vol. 25, S.125-132, 1994

[7] Delgado, I. R., Fatigue Crack Growth Behaviour Evaluation of Grainex Mar-M 247 for NASA´s High Temperature High Speed Turbine Seal Test Ring, Journal of Engineering for Gas Turbines and Power, Vol. 131, ASME, 2009

[8] Scholz, A., Berger, C., Mueller, F.: Long-term crack behaviour under creep and creep-fatigue conditions of heat resistant steels, 5th International Conference on Advances in Materials Technology for Fossil Power Plants, 3.-5. October 2007, Marco Island, Florida, USA

Corresponding author: rudnig@mpa-ifw.tu-darmstadt.de